FERMILAB-PUB-13-104-AE-E

Dark Matter Search Results Using the Silicon Detectors of CDMS II

R. Agnese,[13] Z. Ahmed,[14] A.J. Anderson,[2] S. Arrenberg,[20] D. Balakishiyeva,[13] R. Basu Thakur,[15]
D.A. Bauer,[15] J. Billard,[2] A. Borgland,[18] D. Brandt,[18] P.L. Brink,[18] T. Bruch,[20] R. Bunker,[7] B. Cabrera,[6]
D.O. Caldwell,[10] D.G. Cerdeno,[1] H. Chagani,[17] J. Cooley,[5] B. Cornell,[14] C.H. Crewdson,[3] P. Cushman,[17]
M. Daal,[9] F. Dejongh,[15] E. Do Couto E Silva,[18] T. Doughty,[9] L. Esteban,[1] S. Fallows,[17] E. Figueroa-Feliciano,[2]
J. Filippini,[14] J. Fox,[3] M. Fritts,[17] G.L. Godfrey,[18] S.R. Golwala,[14] J. Hall,[19] R.H. Harris,[8] S.A. Hertel,[2]
T. Hofer,[17] D. Holmgren,[15] L. Hsu,[15] M.E. Huber,[11] A. Jastram,[8] O. Kamaev,[3] B. Kara,[5] M.H. Kelsey,[18]
A. Kennedy,[17] P. Kim,[18] M. Kiveni,[7] K. Koch,[17] M. Kos,[7] S.W. Leman,[2] B. Loer,[15] E. Lopez Asamar,[1]
R. Mahapatra,[8] V. Mandic,[17] C. Martinez,[3] K.A. McCarthy,[2] N. Mirabolfathi,[9] R.A. Moffatt,[6]
D.C. Moore,[14] P. Nadeau,[3] R.H. Nelson,[14] K. Page,[3] R. Partridge,[18] M. Pepin,[17] A. Phipps,[9] K. Prasad,[8]
M. Pyle,[9] H. Qiu,[5] W. Rau,[3] P. Redl,[6] A. Reisetter,[12] Y. Ricci,[3] T. Saab,[13] B. Sadoulet,[9, 16] J. Sander,[8]
K. Schneck,[18] R.W. Schnee,[7] S. Scorza,[5] B. Serfass,[9] B. Shank,[6] D. Speller,[9] K.M. Sundqvist,[9]
A.N. Villano,[17] B. Welliver,[13] D.H. Wright,[18] S. Yellin,[6] J.J. Yen,[6] J. Yoo,[15] B.A. Young,[4] and J. Zhang[17]
(CDMS Collaboration)

[1]*Departamento de Física Teórica and Instituto de Física Teórica UAM/CSIC,*
Universidad Autónoma de Madrid, 28049 Madrid, Spain
[2]*Department of Physics, Massachusetts Institute of Technology, Cambridge, MA 02139, USA*
[3]*Department of Physics, Queen's University, Kingston ON, Canada K7L 3N6*
[4]*Department of Physics, Santa Clara University, Santa Clara, CA 95053, USA*
[5]*Department of Physics, Southern Methodist University, Dallas, TX 75275, USA*
[6]*Department of Physics, Stanford University, Stanford, CA 94305, USA*
[7]*Department of Physics, Syracuse University, Syracuse, NY 13244, USA*
[8]*Department of Physics, Texas A&M University, College Station, TX 77843, USA*
[9]*Department of Physics, University of California, Berkeley, CA 94720, USA*
[10]*Department of Physics, University of California, Santa Barbara, CA 93106, USA*
[11]*Department of Physics, University of Colorado, Denver, CO 80217, USA*
[12]*Department of Physics, University of Evansville, Evansville, IN 47722, USA*
[13]*Department of Physics, University of Florida, Gainesville, FL 32611, USA*
[14]*Division of Physics, Mathematics, & Astronomy,*
California Institute of Technology, Pasadena, CA 91125, USA
[15]*Fermi National Accelerator Laboratory, Batavia, IL 60510, USA*
[16]*Lawrence Berkeley National Laboratory, Berkeley, CA 94720, USA*
[17]*School of Physics & Astronomy, University of Minnesota, Minneapolis, MN 55455, USA*
[18]*SLAC National Accelerator Laboratory/Kavli Institute for Particle*
Astrophysics and Cosmology, 2575 Sand Hill Road, Menlo Park 94025, CA
[19]*Pacific Northwest National Laboratory, Richland, WA 99352, USA*
[20]*Physics Institute, University of Zürich, Winterthurerstr. 190, CH-8057, Switzerland*

We report results of a search for Weakly Interacting Massive Particles (WIMPs) with the silicon (Si) detectors of the CDMS II experiment. A blind analysis of data from eight Si detectors, with a total raw exposure of 140.2 kg-days, revealed three WIMP-candidate events with a final surface-event background estimate of $0.41^{+0.20}_{-0.08}(stat.)^{+0.28}_{-0.24}(syst.)$. Other known backgrounds from neutrons and ^{206}Pb are limited to < 0.13 and < 0.08 events at the 90% confidence level, respectively. These data place a 90% upper confidence limit on the WIMP-nucleon cross section of 2.4×10^{-41} cm^2 at a WIMP mass of 10 GeV/c^2. Simulations indicate a 5.4% probability that a statistical fluctuation of the known backgrounds would produce three or more events in the signal region. A profile likelihood ratio test that includes the measured recoil energies of the three events gives a 0.19% probability for the known-background-only hypothesis when tested against the alternative WIMP+background hypothesis. The highest likelihood was found for a WIMP mass of 8.6 GeV/c^2 and WIMP-nucleon cross section of 1.9×10^{-41} cm^2.

PACS numbers: 14.80.Ly, 95.35.+d, 95.30.Cq, 95.30.-k, 85.25.Oj, 29.40.Wk

There is now overwhelming evidence that the bulk of the matter in our universe is in some nonluminous, nonbaryonic form [1]. Weakly Interacting Massive Particles (WIMPs) [2] form a leading class of candidates for this dark matter. Particles of this type would be produced thermally in the early universe and are predicted by many theoretical extensions to the Standard Model of particle physics [1, 3, 4]. If WIMPs do constitute the dark matter in our galaxy, they may be detectable through their elastic scattering from nuclei in terrestrial particle detectors [5]. Numerous experimental groups have sought to detect such scattering events using a wide variety of technologies [6].

The Cryogenic Dark Matter Search (CDMS) collaboration identifies nuclear recoils (including those that would occur in WIMP interactions) using semiconductor detectors operated at 40 mK. These detectors use simultaneous measurements of ionization and non-equilibrium phonons to identify such events among the far more numerous background of electron recoils. During 2003-2008 the collaboration operated CDMS II, an array of Ge and Si detectors located at the Soudan Underground Laboratory [7]. Previous results from the CDMS II installation [8–11] have set world-leading upper limits on the WIMP-nucleon scattering cross section and constrained some non-WIMP dark matter candidates [12].

The low atomic mass of Si generally makes it a less sensitive target for spin-independent WIMP interactions relative to the larger coherent enhancement of the scattering cross section for heavy nuclei. On the other hand, the lower atomic mass of Si is advantageous in searches for WIMPs of relatively low mass due to more favorable scattering kinematics. A WIMP of mass $\lesssim 40$ GeV/c^2 will transfer more recoil energy to a Si nucleus than a Ge nucleus on average. For a recoil energy threshold of ~ 10 keV, WIMPs of sufficiently low mass ($\lesssim 10$ GeV/c^2) will generate more detectable recoils in a Si detector since the more numerous Ge recoils would fall below the detector threshold. New particles at such masses are generally disfavored in fits of models to precision electroweak data (*e.g.* [13]), but viable models in this regime do exist (*e.g.* [14, 15]). Renewed interest in this mass range has been motivated by results from the DAMA/LIBRA [16], CoGeNT [17], and CRESST [18] experiments, which can be interpreted as evidence of low-mass WIMP scattering.

In its final configuration, the CDMS II array consisted of 30 Z-sensitive ionization and phonon (ZIP) detectors: 19 Ge ($\sim$239 g each) and 11 Si ($\sim$106 g each), for a total of $\sim$4.6 kg of Ge and $\sim$1.2 kg of Si. Each CDMS II detector is a semiconductor disk, 7.6 cm in diameter and 1 cm thick, instrumented to detect the phonons and ionization generated by particle interaction within the crystal [7]. We discriminate nuclear recoils from background electron recoils using the ratio of ionization to phonon recoil energy (ionization "yield"). Electron recoils that occur within $\sim$10 μm of a detector surface can exhibit reduced ionization collection. These events are identified by phonon pulse-shape discrimination. Our overall misidentification rate of electron recoils is less than 1 in 10^6.

We consider data from the Si detectors using the final four run periods of the full CDMS II detector installation, acquired between July 2007 and September 2008. The Ge results from this data set have been described in previous publications [11]. Of the 11 Si detectors, three were excluded from the WIMP-search analysis: two due to wiring failures that led to incomplete collection of the ionization signal and one due to unstable response on one of its four phonon channels. Periods of poor performance, as identified by a series of Kolmogorov-Smirnov tests, were also excluded from analysis. After all such exclusions, the data collected by the 8 Si detectors considered in this analysis represent a total exposure of 140.2 kg-days prior to the application of the WIMP candidate selection criteria.

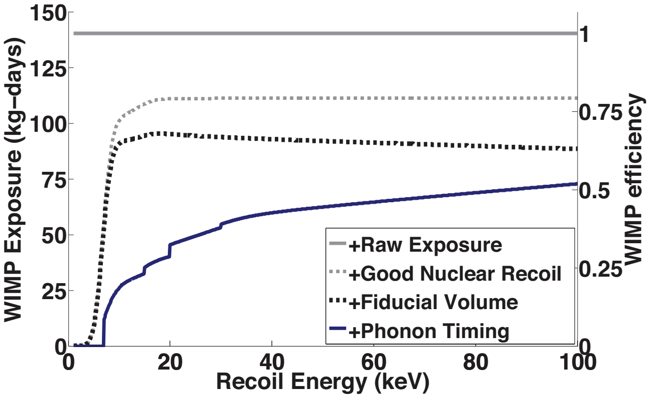

FIG. 1. Exposure (left y axis) and efficiency (right y axis) as functions of recoil energy after application of each WIMP-selection criterion shown. Each curve from top to bottom shows the cumulative effect of successive cuts on the data, such that the bold solid curve shows the overall efficiency of this analysis. The abrupt drops in acceptance at low recoil energies reflect the elevated energy thresholds chosen for some detectors.

The responses of these detectors to electron and nuclear recoils were calibrated using events from extensive exposures to ^{133}Ba and ^{252}Cf sources *in situ* at Soudan. Electron recoils from the former were used to empirically characterize and correct for the dependence of phonon pulse shape on event position and energy. The 356 keV gamma ray from the ^{133}Ba source has a $\sim$ 4.2 cm attenuation length in Si, and thus the Si detectors generally do not show a clear line at 356 keV. Their energy scales were calibrated using 356 keV events with total energies shared between the Si detector and a neighboring detector.

WIMP-candidate events were identified by a series of selection criteria. As with the Ge data analysis, events in and near the WIMP-candidate region were automatically removed from the data set during the analysis, and all WIMP-selection criteria were defined blindly using calibration and remaining WIMP-search data. Thus, WIMP candidates had no impact on the definition of the selection criteria. A WIMP candidate was required to have phonon and ionization signals inconsistent with noise alone in exactly one ZIP detector and to exhibit no coincident energy in the scintillating veto shield or in any of the other 29 ZIP detectors. Events in coincidence with the NuMI beam [19] were also vetoed. We demanded that any candidate event occur within the detector's fiducial volume, defined by requiring signal consistent with noise in the outer ionization electrode. Candidate events were also required to have ionization yield and phonon pulse timing consistent with a nuclear recoil. The recoil energy

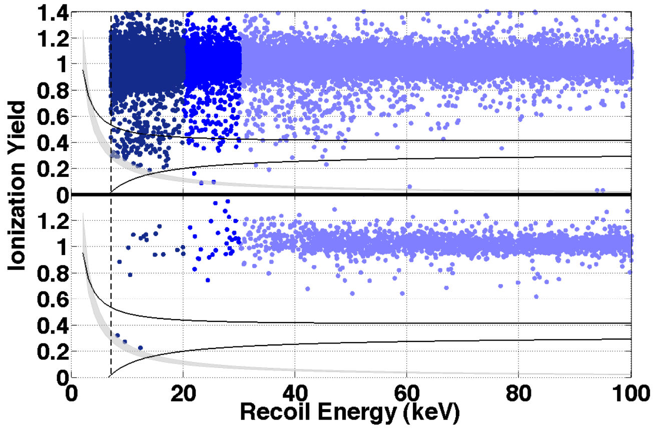

FIG. 2. Ionization yield versus recoil energy in all detectors included in this analysis for events passing all signal criteria except (*top*) and including (*bottom*) the phonon timing criterion. The curved black lines indicate the signal region (-1.8σ and +1.2σ from the mean nuclear recoil yield) between 7 and 100 keV recoil energies, while the gray band shows the range of charge thresholds. Electron recoils in the detector bulk have yield near unity. The data are colored to indicate recoil energy ranges (dark to light) of 7–20, 20–30, and 30–100 keV to aid the interpretation of Fig. 3.

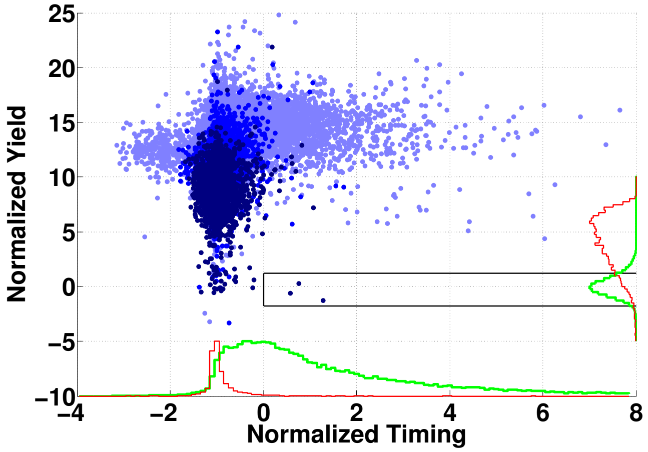

FIG. 3. Normalized ionization yield (standard deviations from the nuclear recoil band centroid) versus normalized phonon timing parameter (normalized such that the median of the surface event calibration sample is at -1 and the cut position is at 0) for events in all detectors from the WIMP-search data set passing all other selection criteria. The black box indicates the WIMP candidate selection region. The data are colored to indicate recoil energy ranges (dark to light) of 7–20, 20–30, and 30–100 keV. The thin red curves on the bottom and right axes are the histograms of surface events from ^{133}Ba calibration data, while the thicker green curves are the histograms of nuclear recoils from ^{252}Cf calibration data.

of each candidate event must lie below 100 keV and above a detector-dependent threshold ranging from 7 to 30 keV, also chosen blindly based on calibration data. In order to take advantage of the fact that the timing parameters are better measured at high energies, the phonon timing data-selection cut was optimized in three energy bins: 7–20 keV, 20–30 keV, and 30–100 keV [20]. Fig. 1 shows the estimated overall exposure to WIMP recoils on the left y-scale, while the right-scale shows the “WIMP efficiency,” namely the estimated fraction of WIMP recoils at a given energy that would be accepted by these signal criteria. The abrupt changes in efficiency are due to the different detector thresholds and changes to the timing cuts in the three energy bins. Signal acceptance was measured using nuclear recoils from ^{252}Cf calibration. Signal acceptance is ∼40% at most recoil energies, somewhat higher than that of the Ge analysis [11]. After applying all selection criteria, the exposure of this analysis is equivalent to 23.4 kg-days over a recoil energy range of 7–100 keV for a WIMP of mass 10 GeV/c^2.

Neutrons from cosmogenic or radioactive processes can produce nuclear recoils that are indistinguishable from those from an incident WIMP. Simulations of the rates and energy distributions of these processes using GEANT4 [21] lead us to expect < 0.13 false candidate events (90% confidence level) in the Si detectors from neutrons in this exposure.

A greater source of background is the misidentification of surface electron recoils, which may suffer from reduced ionization yield and thus contribute events to the WIMP-candidate region; these events are termed “leakage events”. Prior to looking at the WIMP-candidate region (unblinding), the expected leakage was estimated using the rate of single scatter events with yields consistent with nuclear recoils from a previously unblinded dataset [22] and the rejection performance of the timing cut measured on low-yield multiple-scatter events from ^{133}Ba calibration data. Two detectors used in this analysis were located at the end of detector stacks, so scatters on their outer faces could not be tagged as multiple scatters. The multiple-scatter rates on the outer faces of these two detectors were estimated using their single-scatter rates from a previously unblinded dataset presented in [22] and the multiples-singles ratio on the interior detectors. The final pre-unblinding estimate for misidentified surface event leakage into the signal band in the eight Si detectors was $0.47^{+0.28}_{-0.17}(stat.)$ events. This initial leakage estimate informed the decision to unblind.

After all WIMP-selection criteria were defined, the signal regions of the Si detectors were unblinded. Three WIMP-candidate events were observed, with recoil energies of 8.2, 9.5, and 12.3 keV. Two events were observed in Detector 3 of Tower 4, and the third was observed in Detector 3 of Tower 5. The events were well separated in time and were in the middle of their respective tower stacks. Fig. 2 illustrates the distribution of events in and near the signal region of the WIMP-search data set before (*top*) and after (*bottom*) application of the phonon timing criterion. Fig. 3 shows an alternate view of these events, expressed in “normalized” versions of yield and timing that are transformed so that the WIMP acceptance regions of all detectors coincide.

After unblinding, extensive checks of the three candidate events revealed no data quality or analysis issues that would invalidate them as WIMP candidates. The signal-to-noise on the ionization channel for the three events (ordered in increasing recoil energy) was measured to be 6.7σ, 4.9σ, and 5.1σ, while the charge threshold had been set at 4.5σ from the noise. A study on possible leakage into the signal band due to ^{206}Pb recoils from ^{210}Po decays found the expected leakage to be negligible with an upper limit of < 0.08 events at the 90% confidence level. The energy distribution of the ^{206}Pb background was constructed using events in which a coincident α was detected in a detector adjacent to one of the 8 Si detectors used in this analysis. Furthermore, as in the Ge analysis, we developed a Bayesian estimate of the rate of misidentified surface events based upon the performance of the phonon timing cut measured using events near the WIMP-search signal region [22]. Classical confidence intervals provided similar estimates [23]. Multiple-scatter events below the electron-recoil ionization-yield region from both ^{133}Ba calibration and WIMP-search data were used as inputs to this model. The final model predicts an updated surface-event leakage estimate of $0.41^{+0.20}_{-0.08}(stat.)^{+0.28}_{-0.24}(syst.)$ misidentified surface events in the eight Si detectors.

This result constrains the available parameter space of WIMP dark matter models. We compute upper limits on the WIMP-nucleon scattering cross section using Yellin's optimum interval method [24]. We assume a WIMP mass density of 0.3 GeV/c^2/cm^3, a most probable WIMP velocity with respect to the galaxy of 220 km/s, a mean circular velocity of Earth with respect to the galactic center of 232 km/s, a galactic escape velocity of 544 km/s [25], and the Helm form factor [26]. Fig. 4 shows the derived upper limits on the spin-independent WIMP-nucleon scattering cross section at the 90% confidence level (C.L.) from this analysis and a selection of other recent results. The present data set an upper limit of 2.4×10^{-41} cm^2 for a WIMP of mass 10 GeV/c^2. We are completing the calibration of the nuclear recoil energy scale using the Si-neutron elastic scattering resonant feature in the ^{252}Cf exposures. This study indicates that our reconstructed energy may be 10% lower than the true recoil energy, which would weaken the upper limit slightly. Below 20 GeV/c^2 the change is well approximated by shifting the limits parallel to the mass axis by $\sim 7\%$. In addition, neutron calibration multiple scattering effects improve the response to WIMPs by shifting the upper limit down parallel to the cross-section axis by $\sim 5\%$.

A model of our known backgrounds, including both energy and expected rate distributions, was constructed for each detector and experimental run for each of the three backgrounds considered: surface electron recoils, neutron backgrounds, and ^{206}Pb recoils. Simulations of our background model yield a 5.4% probability of a statistical fluctuation producing three or more events in our signal region.

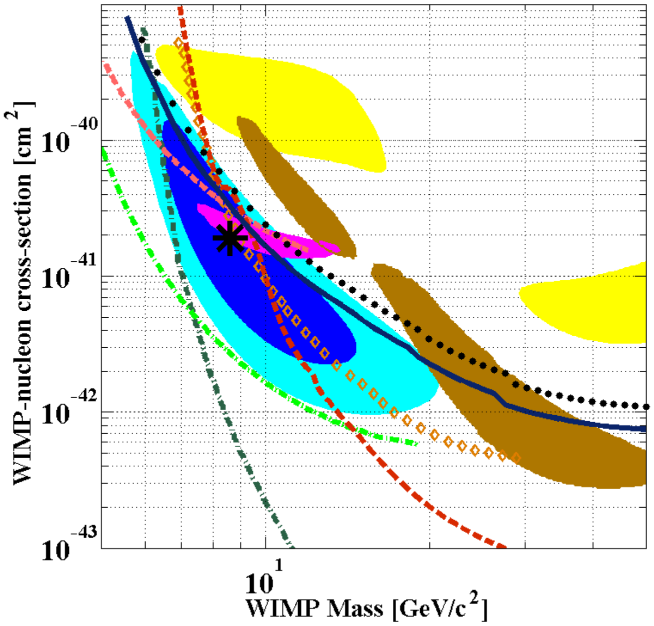

FIG. 4. Experimental upper limits (90% confidence level) for the WIMP-nucleon spin-independent cross section as a function of WIMP mass. We show the limit obtained from the exposure analyzed in this work alone (*black dots*), and combined with the CDMS II Si data set reported in [22] (*blue solid line*). Also shown are limits from the CDMS II Ge standard [11] and low-threshold [27] analysis (*dark and light dashed red*), EDELWEISS low-threshold [28] (*orange diamonds*), XENON10 S2-only [29] (*light dash-dotted green*), and XENON100 [30] (*dark dash-dotted green*). The filled regions identify possible signal regions associated with data from CoGeNT [31] (*magenta*, 90% C.L., as interpreted by Kelso *et al.* including the effect of a residual surface event contamination described in [32]), DAMA/LIBRA [16, 33] (*yellow*, 99.7% C.L.), and CRESST [18] (*brown*, 95.45% C.L.) experiments. 68% and 90% C.L. contours for a possible signal from these data are shown in blue and cyan, respectively. The asterisk shows the maximum likelihood point at (8.6 GeV/c^2, 1.9×10^{-41} cm^2).

This model of our known backgrounds was used to investigate the data in the context of a WIMP+background hypothesis. We performed a profile likelihood analysis in which the background rates were treated as nuisance parameters and the WIMP mass and cross section were the parameters of interest. The highest likelihood is found for a WIMP mass of 8.6 GeV/c^2 and a WIMP-nucleon cross section of $1.9{\times}10^{-41}$ cm^2. The goodness-of-fit test of this WIMP+background hypothesis results in a p-value of 68%, while the background-only hypothesis fits the data with a p-value of 4.5%. A profile likelihood ratio test including the event energies finds that the data favor the WIMP+background hypothesis over our background-only hypothesis with a p-value of 0.19%. Though this result favors a WIMP interpretation over the known-background-only hypothesis, we do not believe this result rises to the level of a discovery.

Fig. 4 shows the resulting best-fit region from this analysis (68% and 90% confidence level contours) on the WIMP-nucleon cross-section vs. WIMP mass plane. The 90% C.L. exclusion regions from CDMS II's Ge and Si analyses and EDELWEISS low-threshold analysis cover part of this best-fit region, but the results are overall statistically compatible. There is much stronger tension with the upper limits from the XENON10 and XENON100 experiments, which exclude the entirety of this parameter space under standard assumptions about the WIMP velocity distribution and WIMP-nucleus interactions.

The CDMS collaboration gratefully acknowledges the contributions of numerous engineers and technicians; we would like to especially thank Dennis Seitz, Jim Beaty, Bruce Hines, Larry Novak, Richard Schmitt and Astrid Tomada. In addition, we gratefully acknowledge assistance from the staff of the Soudan Underground Laboratory and the Minnesota Department of Natural Resources. This work is supported in part by the National Science Foundation (Grant Nos. AST-9978911, NSF-0847342, NSF-1102795, NSF-1151869, PHY-0542066, PHY-0503729, PHY-0503629, PHY-0503641, PHY-0504224, PHY-0705052, PHY-0801708, PHY-0801712, PHY-0802575, PHY-0847342, PHY-0855299, PHY-0855525, and PHY-1205898), by the Department of Energy (Contracts DE-AC03-76SF00098, DE-FG02-92ER40701, DE-FG02-94ER40823, DE-FG03-90ER40569, and DE-FG03-91ER40618, and de-sc0004022), by the Swiss National Foundation (SNF Grant No. 20-118119), by NSERC Canada (Grants SAPIN 341314 and SAPPJ 386399), and by MULTIDARK CSD2009-00064 and FPA2012-34694. Fermilab is operated by Fermi Research Alliance, LLC under Contract No. De-AC02-07CH11359, while SLAC is operated under Contract No. DE-AC02-76SF00515 with the United States Department of Energy.

---

[1] G. Bertone, D. Hooper, and J. Silk, Phys. Rept., **405**, 279 (2005).

[2] G. Steigman and M. S. Turner, Nucl. Phys., **B253**, 375 (1985).

[3] B. W. Lee and S. Weinberg, Phys. Rev. Lett., **39**, 165 (1977).

[4] G. Jungman, M. Kamionkowski, and K. Griest, Phys. Rept., **267**, 195 (1996).

[5] M. W. Goodman and E. Witten, Phys. Rev., **D31**, 3059 (1985).

[6] G. Bertone and J. Silk, *Particle Dark Matter : Observations, Models and Searches* (Cambridge University Press, 2010).

[7] D. Akerib *et al.* (CDMS Collaboration), Phys.Rev., **D72**, 052009 (2005), arXiv:astro-ph/0507190 [astro-ph].

[8] D. S. Akerib *et al.* (CDMS), Phys. Rev. Lett., **93**, 211301 (2004).

[9] D. S. Akerib *et al.* (CDMS), Phys. Rev. Lett., **96**, 011302 (2006).

[10] Z. Ahmed *et al.* (CDMS), Phys. Rev. Lett., **102**, 011301 (2009).

[11] Z. Ahmed *et al.* (CDMS), Science, **327**, 1619 (2010).

[12] Z. Ahmed *et al.* (CDMS), Phys. Rev., **D81**, 042002 (2010); Phys. Rev. Lett., **103**, 141802 (2009).

[13] E. A. Baltz and P. Gondolo, JHEP, **10**, 052 (2004); L. Roszkowski, R. Ruiz de Austri, and R. Trotta, **07**, 075 (2007).

[14] A. Bottino, F. Donato, N. Fornengo, and S. Scopel, Phys. Rev., **D69**, 037302 (2004).

[15] D. E. Kaplan, M. A. Luty, and K. M. Zurek, Phys. Rev., **D79**, 115016 (2009); T. Cohen and K. M. Zurek, Phys. Rev. Lett., **104**, 101301 (2010).

[16] R. Bernabei *et al.* (DAMA), Eur. Phys. J., **C67**, 39 (2010).

[17] C. E. Aalseth *et al.* (CoGeNT), arXiv:1208.5737 (2012).

[18] G. Angloher *et al.* (CRESST), European Physical Journal C, **72**, 1971 (2012), arXiv:1109.0702 [astro-ph.CO].

[19] K. Anderson, B. Bernstein, D. Boehnlein, K. R. Bourkland, S. Childress, *et al.*, (1998).

[20] K. A. McCarthy, Ph.D. thesis, Massachusetts Institute of Technology (2013).

[21] J. Allison *et al.*, Nuclear Science, IEEE Transactions on, **53**, 270 (2006), ISSN 0018-9499.

[22] J. P. Filippini, Ph.D. thesis, University of California, Berkeley (2008), paper to be submitted to PRD.

[23] I. Ruchlin and R. W. Schnee, Nuclear Instruments and Methods in Physics Research A, **664**, 336 (2012), arXiv:1106.6296 [physics.data-an].

[24] S. Yellin, Phys. Rev., **D66**, 032005 (2002).

[25] M. C. Smith, G. Ruchti, A. Helmi, R. Wyse, J. Fulbright, *et al.*, Mon.Not.Roy.Astron.Soc., **379**, 755 (2007), arXiv:astro-ph/0611671 [astro-ph].

[26] J. D. Lewin and P. F. Smith, Astropart. Phys., **6**, 87 (1996).

[27] Z. Ahmed *et al.* (CDMS), Physical Review Letters, **106**, 131302 (2011).

[28] E. Armengaud *et al.* (EDELWEISS), Phys. Rev. D, **86**, 051701 (2012), arXiv:1207.1815 [astro-ph.CO].

[29] J. Angle *et al.* (XENON), Physical Review Letters, **107**, 051301 (2011), arXiv:1104.3088 [astro-ph.CO].

[30] J. Angle *et al.* (XENON), Phys. Rev. Lett., **100**, 021303 (2008).

[31] C. Kelso, D. Hooper, and M. R. Buckley, Phys. Rev. D, **85**, 043515 (2012), arXiv:1110.5338 [astro-ph.CO].

[32] C. E. Aalseth *et al.* (CoGeNT), Physical Review Letters, **107**, 141301 (2011), arXiv:1106.0650 [astro-ph.CO].

[33] C. Savage, G. Gelmini, P. Gondolo, and K. Freese, JCAP, **0904**, 010 (2009).